

A Technique to Retrieve High-Frequency Permeability of Metals from Constitutive Parameters of Composites with Metal Inclusions of Arbitrary Shape, Estimate of the Microwave Permeability of Nickel

Sergey N. Starostenko^{*}, Konstantin N. Rozanov,
Artem O. Shiryaev, and Andrey N. Lagarkov

Abstract—The technique to retrieve the microwave permeability of metals from the measured constitutive parameters of composites with fine powder of these metals is developed. The technique is based on the modified Sihvola mixing rule and describes a wide range of contrasts in the component susceptibility, accounts for both the inclusion shape and the percolation threshold. These parameters are related to the Bergman-Milton shape-distribution width and to composite structure. The technique is applied to retrieve the microwave permeability of nickel. The metal permeability is calculated from the measured permittivity and permeability of paraffin-bound composites filled with nickel flakes or spheres with account for skinning in conducting inclusions. The measurements are performed using the transmission coaxial-cell in the frequency range up to 15 GHz. The effects of filling factor, inclusion shape and size on the retrieved permeability spectra are analyzed. The permeability retrieval procedure is based on parameter fitting of the selected mixing model for the measured permittivity and permeability data. The retrieved permeability is close to the data available from archived literature sources that are obtained with thick nickel wires and foils.

1. INTRODUCTION

Designers of high-frequency devices require the knowledge of the permeability of metals composing these devices. The direct measurement of the microwave permeability of metals is hindered by the low skin depth, which is less than one micrometer at microwave frequencies. The idea to estimate metal permeability from that of a composite filled with fine powder of the metal applying some mixing formula that relates the properties of a powder particle to those of a composite is far from an original one [1, 2]. The novelty of the proposed technique is in selection of the mixing model true for a range of composite structures and in a simultaneous treatment of several independent transport properties of a composite, namely in the simultaneous treatment of parameters describing electric charge and magnetization transport; the parameters are permittivity and permeability. The permittivity is selected here as the second parameter because of two reasons. The first one is that the permittivity can be measured with the same experimental setup and samples together with permeability. The second reason is that the contrast between the permittivity and permeability of mixture components differs significantly. In principle any other transport parameter (say, thermal conductivity, Young's module, etc.) may be treated [3, 4] together with permeability. The measurement of several transport properties of composite samples is necessary because realistic mixing models (the general models that account for inclusion shape and interaction) have several unknown parameters that cannot be determined accurately treating the measured permeability only [5–7].

Received 17 July 2018, Accepted 5 November 2018, Scheduled 6 December 2018

^{*} Corresponding author: Sergey N. Starostenko (snstar@mail.ru).

The authors are with the Institute for Theoretical and Applied Electromagnetics, Russia.

The problem is that the microwave permeability of known magnets is relatively low, and if the permeability contrast of mixture components is low, the physically correct mixing models asymptotically turn to the Landau-Lifshitz-Looyenga formula [8, 9] where the effects of inclusion shape, of mixture structure, etc. are negligible (in the case of one-dimensional composite the Landau-Lifshitz-Looyenga formula is equivalent to the Wiener formula [10]). Therefore, the treatment of microwave permeability of composites without the data on some other transport properties of these composites may lead to selection of a mixing model that incorrectly accounts for inclusion shape and interaction. As a result, the retrieved permeability of inclusion is a formal parameter of the selected model unrelated to metal permeability, which is the critical drawback of known attempts to estimate the microwave permeability of metals [1, 2, 11].

The proposed technique is tested to retrieve the microwave permeability of nickel (Ni). Nickel is selected here as a test object because Ni and Ni-based coatings are widely used in electronic circuits because of high corrosion resistance. At microwaves, the effects of these coatings are difficult to predict. Examples include the effect of Ni coating on loss in coaxial connectors [12] and the enhancement of electromagnetic interference suppression due to Ni coating [13]. The preliminary data retrieved for Ni powders by the technique analyzed here are presented in [14].

Data on microwave permeability of Ni collected in [15] are based on loss study in Ni wires, thick foils, Ni coatings, or bulk conductors. Energy lost by a high-frequency current in a conductor is defined by the product of the electric resistivity ρ and the complex permeability $\mu = \mu' + i\mu''$ of the conductor. The problem of measurements with a thick metal is that the surface resistivity value may differ from that of the DC-measured value of a bulk sample: the surface resistivity is affected by surface roughness, impurities, mechanical stress, etc. Another problem is that the loss measurement accuracy decreases steeply with decreasing frequency, the reported permeability data obtained with thick metal in the GHz frequency range scatter significantly [15].

Theoretical calculations [8, 9] of the permeability of Ni at microwaves based on magnetostatic parameters (saturation magnetization, anisotropy field, etc.) are contradictory and agree poorly with experimental data [15]. Fig. 1 shows the reported real part of the permeability as a function of frequency, where the measured data are shown as symbols, and the simulation data are shown as lines [14].

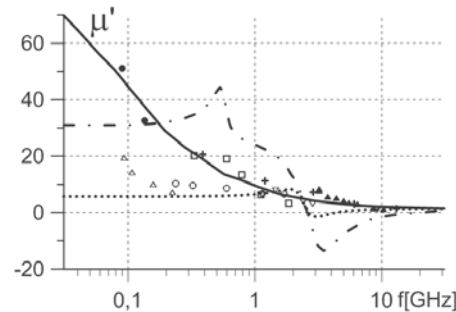


Figure 1. Published data [14] for the microwave permeability of Ni, where the solid and dot-dashed lines show simulation data and the dotted line shows data retrieved from loss in coaxial connectors [12]. The symbols present handbook collected measurements with bulk Ni [15].

Note that the data collected in Fig. 1 are contradictory and are unfit even for a rough estimation of Ni permeability at microwaves.

Permeability measurements on metal particles with size close to the skin depth are less sensitive to the resistivity uncertainty than bulk metals. Despite the fact that particle thickness d and resistivity ρ are rarely known precisely, the value of d/ρ ratio may be determined with reasonable accuracy. This ratio is related to magnetic loss (i.e., to the imaginary part of permeability μ''), so the d/ρ -value may be readily fitted to obtain zero loss at the frequency much lower than the ferromagnetic resonance (FMR) frequency ($\mu'' = 0$ at $f \rightarrow 0$ [5, 6]), see Section 3.

The broadband measurements of the magnetic response of a single particle with a diameter of 1–10 μm are problematic even with modern vector network analyzers because of a low signal to noise

ratio. The response can be increased by measuring an assembly of particles.

The proposed technique is based on the application of a mixing rule to describe the permittivity and permeability dependence for a composite on volume fraction (on filling factor) p of a metal [1, 2, 5, 6, 16, 17].

The permittivity measurements with Ni are more complicated than measurements of composites with iron or sendust powders [5–7], as Ni powders are electrically conductive because of oxide-free particle surface. A thin (less than 2% of inclusion diameter) oxide layer inherent to iron-based alloys suppresses the electric contact between the neighboring particles and decreases the effective permittivity of inclusion down to $\sim 10^3$ [18]; the inclusion in a shell is conventionally considered as a homogeneous substance. The estimates of inclusion permeability based on the comparison of composite permittivity and permeability [5, 6] are valid for metal powders in an oxide shell as the effective permittivity of inclusion ($\sim 10^3$) is still much higher than its permeability.

The Ni-filled composites are DC conductive at the same filling where composites with most permeable metals are insulators. The DC conductivity leads to several specific problems; the permittivity measurement for a low-resistive sample is a difficult experimental task (e.g., the permittivity of metals has only been estimated theoretically up-to-date). Known mixing models relate composite constitutive parameters to those of inclusion with account for inclusion shape, filling factor and composite structure [19], but they do not account for contact effects and, therefore, even the realistic models are highly inaccurate in describing resistance or dielectric loss for composites filled close to the percolation threshold.

The idea of inclusion permeability retrieval developed in this study is similar to that employed in [5, 6], where the permittivity ε and permeability μ data measured for a set of filling factors were treated to fit two mixing models, which are the most different from each other, namely the symmetric Bruggeman model and the Odelevskiy model (the Maxwell Garnett model modified with the account for percolation), see Section 3. The development of the above idea is here based on calculating the inclusion permeability as a function of static dielectric χ_ε and dynamic magnetic χ_μ susceptibilities of composites; the function is defined by a selected mixing model. Note that the dynamic dielectric susceptibility χ_ε is not treated here because of unaccounted for contribution of contact effects (these effects often lead to complicated and poorly reproduced dependence of the measured permittivity on frequency). The Sihvola mixing model [20] is modified and applied here to treat the constitutive parameters determined experimentally. In contrast to the previous publications [5–7], the applied mixing model is more general than the Odelevskiy and Bruggeman models; the Sihvola mixing model describes a range of mixture structures (see Section 3) using the same number of fitted parameters as in publications [5–7] but accounts for the finite linewidth of the geometric spectral function [9, 21, 22]. This linewidth is a function of inclusion shape, filling factor and of composite structure.

The metal permeability is calculated from the fitted permeability of inclusion with the account for skinning in a sphere or in an infinite plane. The results of permeability retrieval are compared with the published data for Ni and with the data obtained using the modified Maxwell Garnett (Odelevskiy) mixing model that describes an idealized crystal-like composite (regular structure of identical inclusions with the delta-shaped geometric spectral function). A reasonable agreement with some of the archived data presented in Fig. 1 is observed.

2. SAMPLE PREPARATION AND MEASUREMENT TECHNIQUE

Commercial grade carbonyl Ni (99.9% Ni) was used as the filler consisting of spherical particles. The median diameter of the particles measured by an Analyzette-22 particle size analyzer is about 12 μm (see Fig. 2).

Ni flakes were prepared by ball milling of spherical powder in ethanol as a cooler and oxidation protector. The milled powder was separated into fractions with two sieves. The composites filled with flakes were prepared using the same 40–63 μm powder fraction as in research with sendust powders [5]. The flake thickness estimated by optical microscopy is about 1–2 μm .

The composites were prepared by mixing the weighted amounts of powder and melted paraffin wax; the mixing was continued until the wax was solidified. Then the mixtures were pressed in the shape of round washers of about 0.5 to 4 mm thick that fit for a standard 7 \times 3 mm coaxial. To keep approximately

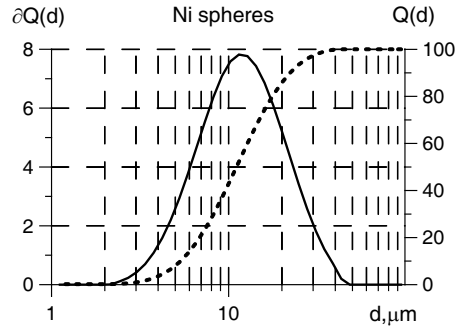


Figure 2. Size distribution $Q(d,)$ presented by dashed line, and size distribution density $\partial Q(d)$ presented by solid line for Ni-spheres determined with Analyzette 22 particle sizer.

the same electrical thickness of the measured sample the washers with lower filling factor have higher thickness. The volume fraction p (the filling factor) of the metal inclusions was verified by density measurements. The above technology results in approximately isotropic samples: the static permittivity of flake-filled samples measured in a washer plane and perpendicular to it shows the difference about 10–30%. The error of the filler content is about 0.5–1% vol.; the error increases with the filling increase. The highest filling obtained by this technology is about 45% Vol. for spheres and about 14% Vol. for flakes. The filling limit is defined by poor mechanical properties and brittleness of pressed washers. The filling of samples under study is several percent lower than the limit as volume fraction of metal inclusions should be below the percolation threshold, where the permittivity contribution of contact effects becomes dominating.

The constitutive parameters of composites were measured similar to article [5] in a coaxial cell applying the Nicolson-Ross-Weir (reflection-transmission) technique within the frequency band from 0.1 to 15 GHz with an Anritzu MS2028 vector network analyzer (VNA). The disassembled coaxial cell together with the washer-shaped sample put on a central conductor is shown in Fig. 3, the coaxial cables are connected to VNA ports. To calculate the sample permittivity and permeability the full set of two-port scattering parameters (S_{11} , S_{12} , S_{22} , S_{21}) is measured at 1024 logarithmically distributed frequency points.

There are two drawbacks with VNA coaxial measurements that make it desired to use a complimentary technique. The first one is that there is an inevitable air gap of about 0.01 to 0.05 mm

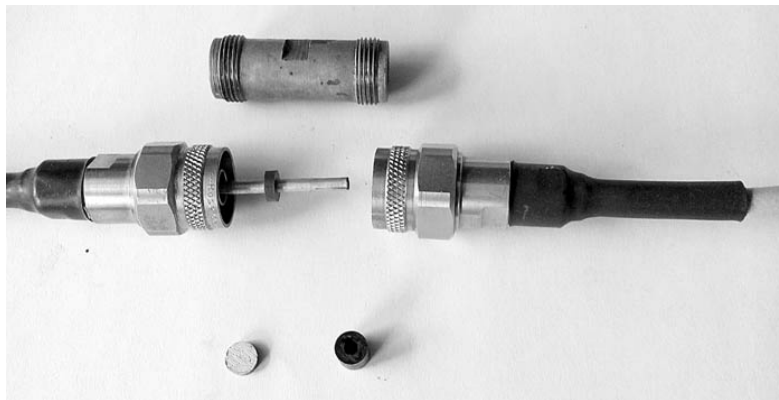


Figure 3. The disassembled transmission coaxial cell and composite samples. The external tube-shaped shell is in the top of the photo. The middle part of the picture shows the washer-shaped sample placed on the central conductor. The right and left rigid coaxial cables are attached to MS2028 VNA ports. The bottom of the picture shows the disk-shaped sample with foil electrodes for quasi-static permittivity measurements and the thick washer-shaped sample for quasi-static permeability measurements.

thick between the washer sample and the cell electrodes (see Fig. 3). The gap forms while the washer is slid into the cell and decreases the accuracy of permittivity measurements; the error becomes critical for samples with high filling. The second drawback is that the electrical thickness of washer-shaped sample is selected to be suitable for a wide frequency band (0.1 to 15 GHz). This electrical thickness is too small for low-frequency quasistatic measurements; the thickness increase may lead to measurement errors due to higher modes in the filled section of coaxial cell [27]. Therefore the quasistatic constitutive parameters were determined using the complimentary technique, namely, the lumped capacity and lumped inductance were measured with an E7-28 immittance analyzer.

In the case of permittivity measurements the aluminum foil electrodes were pressed to disk samples to decrease the errors because of the air gaps inherent to coaxial measurements. The disk samples (of 7 mm diameter and of about 0.4 to 1.2 mm thickness) were repressed together with the foil electrodes from the washer-shaped samples previously used for coaxial measurements.

The lumped inductance measurements were performed comparing the inductance of 5 cm-long piece of wire and the inductance of the same wire with 7×3 mm composite washers of total thickness about 10–15 mm.

The obtained capacity and inductance data were median filtered to decrease the measurement error in the frequency range 1–10 MHz and used with account of sample dimensions to calculate the quasistatic permittivity and permeability values.

3. APPLICATION OF THE SIHVOLA FORMULA TO RETRIEVE INCLUSION PERMEABILITY

The technique to retrieve the dependence of the intrinsic permeability of Ni on frequency is based on simultaneous treatment of permittivity and permeability data similarly to [5]. However, a set of two mixing models is substituted here with a single formula comprising several mixing models, namely with the Sihvola formula [20]:

$$\frac{\chi_{32}}{\chi_{12}} = p \frac{\sum_{k=1}^3 \frac{1 + a\chi_{32}}{1 + a\chi_{32} + N_k\chi_{12}}}{3 - p\chi_{12} \sum_{k=1}^3 \frac{N_k}{1 + a\chi_{32} + N_k\chi_{12}}} \quad (1)$$

Here the original formula [20] is written in terms of susceptibility normalized to permittivity or permeability of a host media; the indexes 1, 2 and 3 refer to metal inclusion, paraffin binder, and composite respectively, χ_{12} is the inclusion susceptibility normalized to permittivity ε_2 or permeability μ_2 of a binder (paraffin wax with $\varepsilon_2 \approx 2.3$, $\mu_2 = 1$), thus χ_{32} is the composite susceptibility also normalized to that of a binder, a is the Sihvola parameter related to the mixture structure, and N is the inclusion shape-factor (the depolarization or demagnetization factor). In the case of dielectric susceptibility, $\chi_{\varepsilon 32} = \varepsilon_1/\varepsilon_2 - 1$ and $\chi_{\varepsilon 32} = \varepsilon_3/\varepsilon_2 - 1$; in the case of magnetic susceptibility, $\chi_{\mu 12} = \mu_1 - 1$ and $\chi_{\mu 32} = \mu_3 - 1$, as $\mu_2 = 1$.

The sum of depolarization factors is equal to unity ($N_1 + N_2 + N_3 = 1$); therefore if the inclusion shape is assumed to be close to that of ellipsoid of rotation ($N_1 + 2N_2 = 1$), Eq. (1) can be written as

$$\frac{\chi_{32}}{\chi_{12}} = p \frac{\frac{1 + a\chi_{32}}{1 + a\chi_{32} + N\chi_{12}} + 2 \frac{1 + a\chi_{32}}{1 + a\chi_{32} + 0.5 \times (1 - N)\chi_{12}}}{3 - p\chi_{12} \left[\frac{N}{1 + a\chi_{32} + N\chi_{12}} + \frac{2 \times 0.5 \times (1 - N)}{1 + a\chi_{32} + 0.5 \times (1 - N)\chi_{12}} \right]} \quad (2)$$

And if the depolarization factor is small ($N \rightarrow 0$, the case of a long fiber or of a flat disk) it is possible to neglect the polarizability contribution of inclusions perpendicular to electric or magnetic field (of inclusions with $1 - N \rightarrow 1$) by account for effective volume fraction of inclusions parallel to the field. In the case of cylinders or fibers, the effective volume fraction is $p_{eff} = p/3$; in the case of disks or flakes, the effective volume fraction is $p_{eff} = 2p/3$. In the case of inclusions close to spheres, the effective volume fraction is equal to the real one $p_{eff} = p$. Therefore, for oblate ellipsoids of rotation

(thin disks) the terms corresponding to polarizability perpendicular to flake plane are negligible, and Eq. (2) is simplified as

$$p_{eff} \frac{\chi_{12}}{\chi_{32}} - 1 = N \chi_{12} \frac{1 - p_{eff}}{1 + a \chi_{32}} \quad (3)$$

By varying the value of a , Eq. (3) may be simplified into the Maxwell Garnett formula (for $a = 0$), into the coherent potential formula (for $a = 1$), into the Bruggeman formula (for $a = 1 - N$), into the Wiener formula (for $a \rightarrow \infty$) [19] and into the Odelevskiy formula (for $a = N(p_c^{-1} - 1)$ and $\chi_{12} \gg \chi_{32}$) [6]:

$$\chi_{32} = \frac{p}{(1 - p/p_c) N + 1/\chi_{12}} \underset{\chi_{12} \rightarrow \infty}{\approx} \frac{p}{(1 - p/p_c) N}, \quad (4)$$

where p_c is the critical volume fraction of metal (the percolation threshold).

Note that the Odelevskiy formula (Eq. (4)) describes a mixture below the percolation threshold and accounts for the identical shape for all inclusions, similarly to the Maxwell Garnet formula. Obviously, Eq. (4) is the particular case of Eq. (3) valid for high contrast of component susceptibilities within the filling range $0 < p < p_c$.

For flakes approximated as oblate ellipsoids of rotation (note that it is a rough approximation, as real flakes are not round as disks), the form-factor N ($0 < N < 1/3$) is defined by Eq. (5) [21]:

$$N = \frac{1}{2} - \frac{1}{2 - 2(d/D)^2} \times \left[1 - \frac{d/D}{\sqrt{1 - (d/D)^2}} \times \text{ArcCos} \left(\frac{d}{D} \right) \right], \quad (5)$$

where D and d are the big and small axes of ellipsoid respectively.

Parameter a in Eq. (3) defines the distribution of inclusion effective shape-factors as the function of filling p (the Bergman-Milton geometrical spectral function [9, 21]).

The composite susceptibility may be obtained by solving Eq. (3) (the solution below corresponds to positive loss in a composite filled below the percolation threshold) as

$$\chi_{32} = \frac{-(1 + N \chi_{12} - a p_{eff} \chi_{12} - N p_{eff} \chi_{12}) + \sqrt{4 a p_{eff} \chi_{12} + (1 + N \chi_{12} - a p_{eff} \chi_{12} - N p_{eff} \chi_{12})^2}}{2a} \quad (6)$$

There are several methods to calculate the shape-factor distribution density function [9, 21–24]. In the case of modified Sihvola mixing model, the function may be calculated analytically using the Ghosh-Fuchs technique [23] from the composite susceptibility (Eq. (6))

$$\begin{aligned} b(n) &= \frac{1}{\pi p} \text{Lim}_{z \rightarrow 0} \left[\text{Im} \left[\frac{-(n + a p_{eff} - N(1 - p_{eff}) + is) + \sqrt{(n + a p_{eff} - N(1 - p_{eff}) + is)^2 - 4 a p_{eff} (n + is)}}{2a(n + is)} \right] \right] \\ &= \frac{\sqrt{4 a p_{eff} n - (n - N(1 - p_{eff}) + a p_{eff})^2}}{2 \pi a n p_{eff}} \end{aligned} \quad (7)$$

Here N is the depolarization factor defined by inclusion shape only, n the running depolarization factor, and $b(n)$ the shape-factor density function. Note that the shape-factor distribution density (the geometrical spectral function) depends on inclusion shape and on structure parameter a . The geometrical spectral functions calculated from Eq. (7) for composites filled with spherical and disk-like inclusions (N - and a -values are selected to be close to the corresponding parameters determined experimentally, see Section 4) are shown in Figs. 4 and 5.

The lower is the inclusion depolarization factor and higher is the value of structure parameter a in Eq. (3), the wider becomes the geometrical spectral function with filling increase. The filling p_{eff} where the distribution width of inclusion shapes becomes infinite (where the minimal depolarization factor becomes equal to zero) corresponds to the percolation threshold (see line $p = 0.43$ in Fig. 4 and line $p = 0.13$ in Fig. 5).

To simplify the calculations therein below we write p instead of p_{eff} , minding the difference defined by inclusion shape (see comments to Eq. (2)).

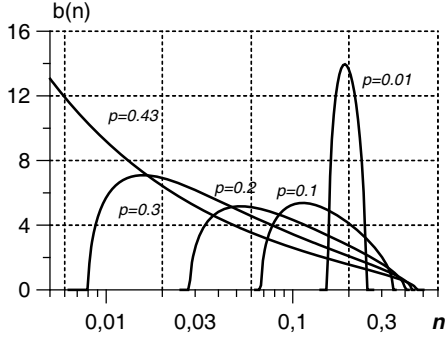


Figure 4. Depolarization factor density distribution (Bergman-Milton spectral functions) for approximately spherical inclusions ($N = 0.2$) with structure parameter $a = 0.27$ and filling factors $p = 0.01, 0.1, 0.2, 0.3, 0.43$.

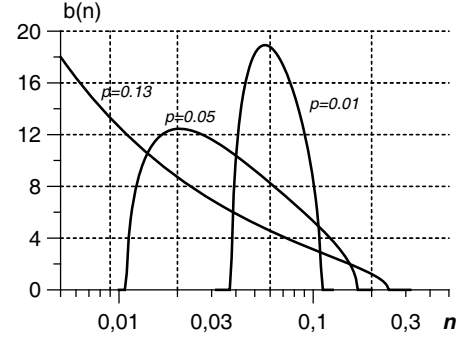


Figure 5. Depolarization factor density distribution (Bergman-Milton spectral functions) for flakes ($N = 0.07$) with structure parameter $a = 0.47$, and filling factors $p_{eff} = 0.01, 0.05, 0.13$.

The percolation threshold p_c is clearer to understand and simpler to determine experimentally in the case of high susceptibility contrast of mixture components than the Sihvola parameter a , therefore Eq. (3) can be rewritten to account for $a = N(p_c^{-1} - 1)$:

$$p \frac{\chi_{12}}{\chi_{32}} - 1 = (1 - p) \frac{N\chi_{12}}{1 + N(1 - p_c^{-1})\chi_{32}}, \quad (8)$$

The modified Sihvola formula (Eq. (8)) describing the dielectric susceptibility for composites with electrically conductive inclusions ($\chi_{\varepsilon 12} = (2\pi f \varepsilon_0 \rho)^{-1}$, here $\varepsilon_0 = 8.85 \times 10^{-12} F/m$) transforms for the filling range where $\chi_{\varepsilon 32} \ll \chi_{\varepsilon 12}$ and $\chi_{\varepsilon 32} \rightarrow \infty$ into the Odelevskiy formula (Eq. (4)) where the composite permittivity depends on inclusion shape and volume fraction only ($\chi_{\varepsilon 32}$ does not depend on $\chi_{\varepsilon 12}$).

The magnetic susceptibility of metals is much lower than the electric susceptibility $\chi_{\mu 12} \ll \chi_{\varepsilon 12}$. Therefore, the composite permeability $\chi_{\mu 32}$ is sensitive to inclusion permeability $\chi_{\mu 12}$ in a wide filling range, and the inclusion permeability $\mu_1 = \chi_{\mu 12} + 1$ can be found as one of the fitted parameters in Eq. (4) together with p_c and N . Note that the values of p_c and N are constant for a selected inclusion shape, whereas the value of $\chi_{\mu 12}(f)$ is frequency dependent. The fitting procedure minimizes the root mean square (RMS) deviation of the calculated $\chi_{\varepsilon 32}$ and $\chi_{\mu 32}$ values from the measured static dielectric susceptibility $\chi_{\varepsilon 32}$ and dynamic magnetic susceptibility $\chi_{\mu 32}(f)$ for samples filled below the percolation threshold ($p < p_c$): $\Sigma(\Delta\mu_{32})^2 + \Sigma(\Delta\varepsilon_{32})^2$. The fitting procedure is applied to the whole set of filling factors p summed over all frequency points f , where the mixture permeability $\mu_3 = \mu'_3 + i\mu''_3$ is measured.

The retrieval error of inclusion susceptibility may be estimated using the procedure proposed in Ref. [5]. Taking a derivative of inclusion susceptibility χ_{32} by composite susceptibility χ_{32} and assuming that $\chi_{12} \approx \chi_{32}/p$ (see Eq. (3)) it is possible to calculate for a given measurement error $\Delta\chi_{32}$ the effect of form factor N and filling p on inclusion susceptibility error $\Delta\chi_{12}$

$$|\Delta\chi_{12}| = \frac{1}{p} \left[\frac{1 + N \left(1 - \frac{p}{p_c}\right) \chi_{12}}{1 - N \left(1 - \frac{p}{p_c}\right) \frac{\chi_{32}}{p}} \right]^2 \times |\Delta\chi_{32}| \approx \frac{1}{p} \left[\frac{1 + N \left(1 - \frac{p}{p_c}\right) \chi_{12}}{1 - N \left(1 - \frac{p}{p_c}\right) \chi_{12}} \right]^2 \times |\Delta\chi_{32}| \quad (9)$$

Equation (9) shows that the retrieval error $\Delta|\chi_{12}|$ is approximately proportional to composite dilution $1/p$, shape factor N and inclusion susceptibility χ_{12} ; therefore, the higher is the filling factor p and the more inclusion shape differs from sphere (the more oblate or vice a verse the more prolate is the inclusion), the lower is the retrieval error for the same measurement error of composite permeability. Note that the retrieval error $\Delta|\chi_{12}|$ grows with inclusion susceptibility χ_{12} (it is obviously impossible to retrieve the electric conductivity of metal inclusion from microwave permittivity measurements); therefore, the permeability error $\Delta|\mu_{12}|$ grows with frequency decrease accordingly to permeability increase due to frequency dispersion.

4. MEASUREMENT RESULTS

The measured dependence of quasistatic dielectric susceptibility $\chi_{\varepsilon 32}$ of composites on filling is shown in Fig. 6. The symbols (the circles for spheres and the squares for flakes) show the measured values, and the lines present the data fit with Eq. (3). The measured dependence of quasistatic magnetic susceptibility $\chi_{\mu 32}$ on filling is shown in Fig. 6. The dotted lines present the permeability approximation using Eq. (3); the solid lines present the approximation with Eq. (4). For permittivity (Fig. 6), the two mixing models are identical below the percolation threshold. The difference should reveal itself close to the percolation threshold, where the permittivity measurements are problematic. For $p \geq p_c$, the samples become resistive and macroscopically inhomogeneous because the conductivity is defined by a few clusters penetrating the measured washer. The inhomogeneity leads to measurement errors and to poor reproducibility due to local filling fluctuations. It is important to note that the measurement error increases for increasing permittivity due to small air gaps between the sample and electrodes.

The measured dependence of quasistatic magnetic susceptibility $\chi_{\mu 32}$ of composites on filling is shown in Fig. 7.

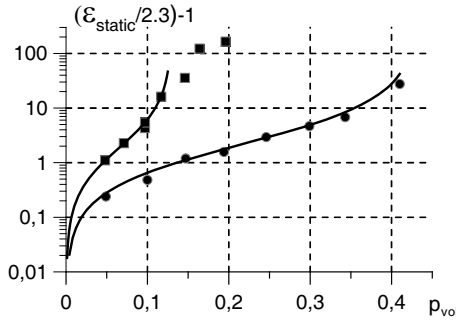


Figure 6. Dependence of static dielectric susceptibility on filling for Ni flakes (squares) and spheres (circles). The lines show approximation using Eq. (4) (for spheres $a = 0.27$, $N = 0.2$, $p_c = 0.43$, for flakes $a = 0.47$, $N = 0.07$, $p_c = 0.13$).

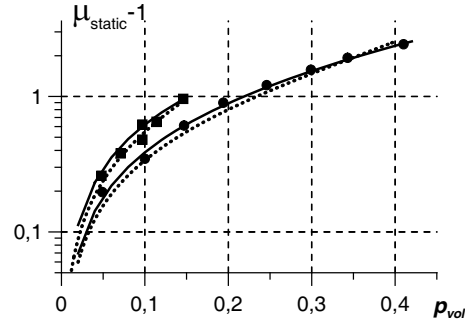


Figure 7. Dependence of static magnetic susceptibility on filling for Ni flakes (squares) and spheres (circles). The solid lines present approximation using Eq. (4) (for spheres $a = 0.27$, $N = 0.2$, $p_c = 0.43$, $\mu_{static_Ni} = 9.5$, for flakes $a = 0.47$, $N = 0.07$, $p_c = 0.13$, $\mu_{static_Ni} = 9$, the values of a , N and p_c are taken here from the permittivity approximations shown in Fig. 6). The dotted lines present the permeability approximation using Eq. (3) (for spheres $\mu_{static} = 8$, for flakes $\mu_{static_Ni} = 7$) Permittivity approximations are identical for both Eq. (3) and Eq. (4).

The measured dependence of permeability on frequency for composites with Ni spheres is shown in Fig. 8, and that with Ni flakes is shown in Fig. 9.

The measured data presented in Fig. 9 with dashed lines are omitted from the fitting procedure (Section 3) as the filling in these samples is close to and above the percolations threshold, where the measured permittivity is affected strongly by contact effects and has poor reproducibility (see Fig. 6). Therefore, the simultaneous treatment of both constitutive parameters measured in the threshold vicinity may lead to errors in parameter fitting and in retrieved permeability of flakes.

5. RETRIEVED PERMEABILITY OF NI

The results of the fitting procedure described in Section 3 and applied to the measured data presented in Fig. 6 and Figs. 8, 9 are the percolation threshold p_c , shape factor N and the retrieved permeability

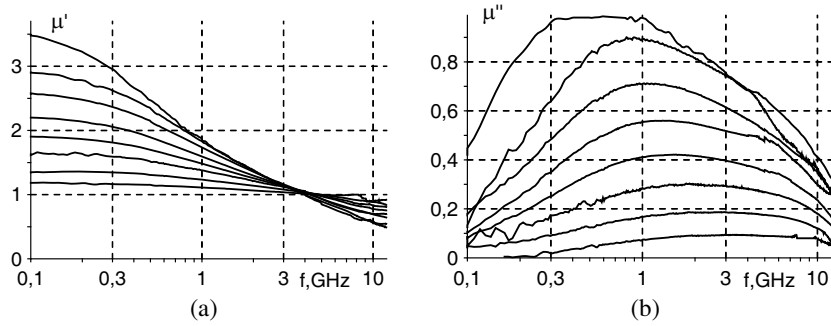


Figure 8. Real (Fig. 8(a)) and imaginary (Fig. 8(b)) permeability dependence on frequency for sphere-filled composites. The measurements are performed with the samples filled as marked by circles in Figs. 6, 7. The filling factors are $p = 0.05, 0.10, 0.15, 0.19, 0.25, 0.30, 0.34, 0.41$; the higher filling p corresponds to higher maximal μ' and μ'' values.

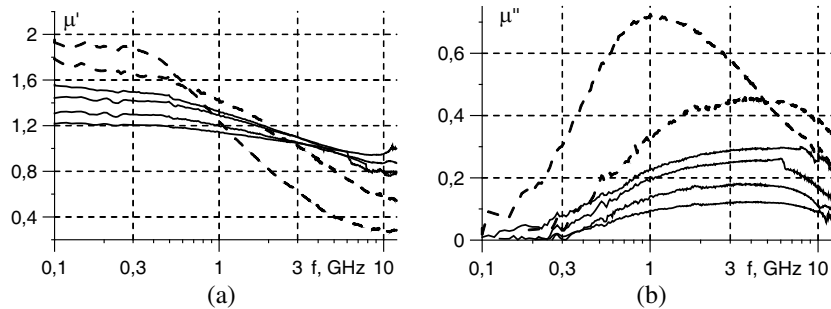


Figure 9. Real (Fig. 9(a)) and imaginary (Fig. 9(b)) permeability dependence on frequency for flake-filled composite. The measurements are performed with the samples filled as marked by squares in Figs. 6, 7. The filling factors are $p = 0.015, 0.068, 0.098, 0.117$ (and $0.146, 0.174$ — dashed lines); the higher filling p corresponds to higher maximal μ' and μ'' values.

data for spherical and flaked inclusions. The fitted permeability of inclusions is presented by curves in Fig. 10. The error bars are calculated with account for 1% measurement error in $\chi_{\mu 32}$; the error estimation for coaxial-line measurements may be found in Ref. [27].

For spherical inclusions, the parameters for Eqs. (3), (4) are: $N = 0.2, p_c = 0.43, a = 0.27$, and $\mu_{static} = 9.5$. For flakes, the parameters are: $N = 0.07, p_c = 0.13, a = 0.47$, and $\mu_{static} = 9$. The values of the depolarization factors are in good agreement with theoretical estimations based on the inclusion shape determined optically (see Section 2): for oblate ellipsoids with diameter $D = 50 \mu\text{m}$ and thickness $d \approx 2 \mu\text{m}$, the depolarization factor is $N \approx 0.03$; for spheres the factor is $N = 0.33$. The difference between the fitted and shape-defined N -values may be related to agglomeration of several neighboring particles [25].

Looking at the error bars in Fig. 10 it may seem that the retrieval of metal permeability with spherical inclusions is more accurate than with flakes. The conclusion is erroneous as the mean diameter of spheres here significantly exceeds the skin-depth and the account for skinning is rather rough because the inclusions are distributed in size and in effective shape (see Figs. 2 and 4).

The skinning contribution may be accounted for by using handbook data for the nickel conductivity ($1.47 \times 10^7 \Omega^{-1}\text{m}^{-1}$) [7] and the inclusion thickness d is estimated microscopically; it is therefore possible to calculate the intrinsic permeability of the metal comprising the inclusion $\mu_{metal}(f)$ excluding skinning.

The skinning is numerically accounted for sphere and for infinite plane [8]. The inclusion permeability is related to that of the comprising metal through the correcting factor $\varphi(\theta)$, which is a function of inclusion electric thickness $\theta = 2\pi f d \sqrt{\varepsilon\mu}$.

For a flake considered as an infinite plane, the factor is

$$\varphi(\theta) = \text{Tan}(\theta) / \theta. \tag{10}$$

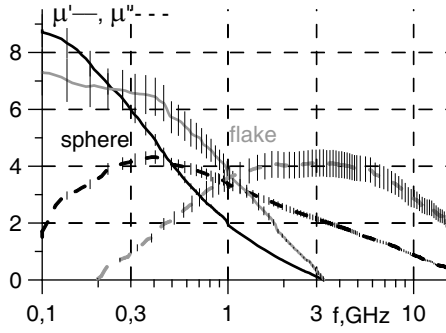


Figure 10. Dependence of sphere permeability (black lines), and flake permeability (grey lines) on frequency. Solid lines present real permeability, dashed lines present imaginary permeability. The error bars are calculated using Eq. (9) for 1% measurement error in $\chi_{\mu 32}$.

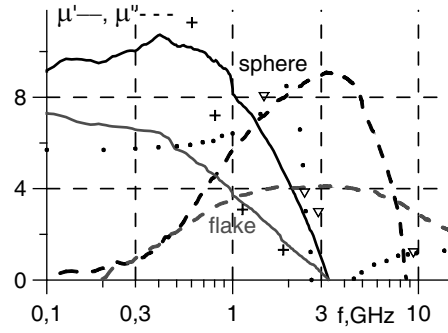


Figure 11. Dependence of metal permeability calculated with account for skinning from sphere permeability (black lines) and flake permeability (grey lines) on frequency. Solid lines present real permeability, dashed lines present imaginary permeability. The crosses, triangles and dots present the data (shown also in Fig. 1) published in Refs. [12, 27, 28] correspondingly.

For a sphere the correcting factor is

$$\varphi(\theta) = 2 [\text{Tan}(\theta) - \theta] / [(\theta^2 - 1) \times \text{Tan}(\theta) + \theta]. \quad (11)$$

The problem is that an error in either inclusion thickness or in its electric conductivity can affect the correcting factor $\varphi(\theta)$ (Eqs. (9), (10)) and consequently the retrieved permeability of the metal. To decrease the effect of uncertainty in θ -value, the inclusion size d used in Eqs. (5), (6) is taken from microscopy measurements (see Section 2), but the conductivity is fitted to obtain zero magnetic loss at low frequency. The fitted conductivity is about 7 times lower than the handbook value. This may be related to the defective structure of the particles compared to bulk Ni. Another problem with skinning is that Eqs. (9), (10) are valid for a particle with well defined size whereas the samples under study are filled with inclusions distributed in size. The neglect of size distribution may lead to negative loss at $f > 10$ GHz (see Fig. 8)

The flake thickness ($\sim 2 \mu\text{m}$) is smaller than the skin depth calculated for the same conductivity as in Ni spheres; the flake permeability presented in Fig. 10 with grey lines is therefore equal to the intrinsic permeability of the metal comprising the flake (Fig. 11).

6. CONCLUSIONS

The described technique to retrieve the microwave permeability of metal from the measured constitutive parameters of composites with the fine powders of the metal is significantly improved compared to known prototypes [1, 2, 5–7, 11, 26].

The main improvement is that the mixing model applied here is valid for a range of mixture structures, therefore the model parameters (particularly, the inclusion permeability) are closer to reality than a formal parameter of some mixing formula unverified for a composite under study.

The second improvement is that the mixing model is verified here by simultaneous treatment of the dependence of two independent parameters on filling, namely of composite permittivity and permeability. The permittivity of metal-insulator mixture is much more sensitive to composite structure than permeability. An incorrect mixing model may seem accurate to describe the measured permeability data, but it leads to an obvious discrepancy between the measured and calculated permittivity data.

The certain advantage is that the Sihvola mixing model applied here is reasonably accurate using three fitted parameters only. These parameters are similar to that of the Odelevskiy model, namely, the inclusion permeability μ_1 , the inclusion shape-factor N and either the percolation threshold p_c or the Sihvola parameter $a = N(p_c^{-1} - 1)$ [19, 20]. The parameters p_c or a are related to inclusion interaction

that defines the dependence of the effective shape factor on filling ($N(p)$). In contrast to the Odelevskiy model where ($N(p)$) is the delta function of filling. In the case of the Sihvola model, these parameters define the distribution density of shape factors $b(n)$ (the width of Bergman-Milton spectral function, see Figs. 4, 5), and $b(n)$ is a function of filling p as well. Here, it is appropriate to cite Ghosh and Fuchs [23]: “It would seem that not much can be deduced from the spectral representation unless we already know the answers. But even in a composite system with an unknown structure, an educated guess on the form of spectral function $b(n)$ gives reasonably good agreement with experiment.” Even the rough account for non-zero width of spectral function proposed here shows that the width of absorption line of composite (see Figs. 8(b), 9(b)) depends on filling and is close to that of inclusion in very diluted mixtures only [26]. The Odelevskiy formula describes the dependence of absorption frequency on filling, but neglects in contrast to the Sihvola formula the shape difference of absorption lines of composite and of filling inclusions.

The higher is the volume fraction of inclusions, the less permeable are the inclusions, the more inclusion shape differs from sphere, the lower is the error of metal permeability retrieval.

The data on permittivity of low-filled composites define the effective shape of metal inclusions; the permittivity of high-filled composites defines the inclusion interaction. This very interaction is related to the Bergman-Milton spectral function and consequently to the selection of the true mixing model. If the inclusion shape and interaction are determined, then the permeability of high-filled composites can be used to retrieve the inclusion permeability.

The developed retrieval technique has several limitations.

An obvious one is the unknown mixing model that relates the permeability of metal particle to that of the composites under study. Therefore the more general is the selected mixing model (the more mixture structures it can describe), the closer are the model parameters to that of composites under study.

The second limitation is that the magnetic and electric properties of fine particles may differ from that of bulk metal; furthermore, the ball-milling can increase this difference. This limitation makes it a fundamental problem to find some standard powders with known spectra of intrinsic permeability to verify the retrieval technique.

The third limitation is that the analytical method of accounting for skinning is developed only for sphere or for infinite plane, and the correcting factor is related to inclusions of identical size, whereas the real composites are filled with inclusions distributed both in size and shape.

The last limitation results from the measurement error of filling factor and constitutive parameters.

The permittivity measurement is simple for composites filled with inclusions in an insulating shell. The less accurate is the proposed permeability retrieval technique, the thicker is the insulating shell than inclusion size. In this study, there is no shell at all, but for a low-resistive sample, the permittivity determination is a problem, and the above measurements are limited to samples with $p < p_c$.

The properties of the metal powder and that of bulk metal may differ significantly. The specific resistance for carbonyl nickel fitted in this work ($8 \times 10^{-5} \Omega \times \text{m}$) accounting for skinning is an order higher than the handbook data ($6.8 \times 10^{-6} \Omega \times \text{m}$) for Ni; the estimated static permeability (~ 10) is also significantly lower than the static permeability (300–600) reported for bulk Ni [7].

The fitted values of static permeability for flakes and spheres are approximately the same, whereas the magnetic absorption line for nickel in flakes shows a high frequency component unobserved for nickel in spheres. The similar effect reported for sendust flakes is related to the dependence of ferromagnetic resonance frequency on inclusion shape [5]. The fundamental conclusion is that the dynamic permeability is undefined for metal as it may depend on the shape of the metal inclusion as well as by its composition.

Note that the calculations with Eq. (3) and Eq. (4) (see Fig. 7) refer to different mixing models and should significantly differ for $p \geq p_c$. The problem is that above the threshold, Eq. (3) is invalid, whereas Eq. (1) is inaccurate because of the contact phenomena that fall out of the scope of the model. Both equations give neighboring estimations of the permeability of Ni at microwave frequencies; the frequency dispersion curves of Ni permeability retrieved from that of spheres and flakes (see Fig. 11) are close to published data obtained with loss measurements for Ni wires and films presented in Fig. 11 by crosses [28] and by empty inverted triangles [29]. Therefore, the Sihvola and the Odelevskiy models are often difficult to distinguish in practice.

ACKNOWLEDGMENT

Support by the Russian Science Foundation grant No. 16-19-10490 is acknowledged.

REFERENCES

1. Olmedo, L., G. Chateau, C. Deleuze, and J. L. Forveille, "Microwave characterization and modelization of magnetic granular materials," *J. Appl. Phys.*, Vol. 73, 6992, 1993.
2. Lederer, P. and C. Brewitt-Taylor, "Measurement of microwave properties of magnetic particulate composites," *IEEE Proc. SCI. Meas. Techn.*, Vol. 147, No. 4, 209, 2000.
3. Odelevskiy, V. I., "Generalized conductivity of heterogeneous systems," Ph.D. Thesis, Leningrad, 1947 (in Russian).
4. Pal, R., *Electromagnetic, Mechanical and Transport Properties of Composite Materials*, CRC Press, Taylor & Frances, London, New-York, 2015.
5. Starostenko, S. N., K. N. Rozanov, A. O. Shiryaev, A. N. Shalygin, and A. N. Lagarkov, "Determination of sendust intrinsic permeability from microwave constitutive parameters of composites with sendust spheres and flakes," *J. Appl. Phys.*, Vol. 121, 245107–245123, 2017.
6. Starostenko, S. N., K. N. Rozanov, A. O. Shiryaev, A. N. Lagarkov, and A. N. Shalygin, "Selection of a mixing model and determination of inclusion microwave permeability for a composite filled with metal powder," *J. Magn. Magn. Mater.*, Vol. 459, 305–310, 2018.
7. Starostenko, S. N., et al., "Estimation of the superhigh-frequency magnetic permeability of alsifer from the measured permeability of composites," *Physics of the Solid State*, Vol. 59, No. 11, 2203–2210, 2017.
8. Landau, L. D., L. P. Pitaevskii, and E. M. Lifshitz, *Electrodynamics of Continuous Media*, Butterworth-Heinemann, Oct. 1984.
9. Tuncer, E., "The Landau-Lifshitz/Looyenga dielectric mixture expression and its self-similar fractal nature," arXiv:cond-mat/0503750, 2005.
10. Wiener, O., *Der Abhandlungen der Mathematisch-Physischen Klasse der Königl. Sächsischen Gesellschaft der Wissenschaften*, 32, 509, 1912.
11. Lagarkov, A. N., V. N. Semenenko, V. A. Chistyayev, and I. T. Iakubov, "High-frequency modes in magnetic spectra of carbonyl iron," *J. Magn. Magn. Mater.*, Vol. 324, 3402–3405, 2012.
12. Shlepnev, Yu. and S. McMorro, "Nickel characterization for interconnect analysis," *IEEE International Symposium on Electromagnetic Compatibility*, 524–529, Aug. 2011.
13. Zivkovic, I. and A. Murk, "Characterization of magnetically loaded microwave absorbers," *Progress In Electromagnetics Research B*, Vol. 33, 277–289, 2011.
14. Starostenko, S. N., K. N. Rozanov, A. O. Shiryaev, V. A. Garanov, and A. N. Lagarkov, "Permeability of nickel determined from microwave constitutive parameters of composites filled with nickel powders," submitted to *IEEE Trans. Magn.*, doi 10.1109/TMAG.2018.2852366.
15. Bozorth, R. M. and N. Y. Ferromagnetism, D. Van Nostrand Co. Inc., 1951.
16. Galek, T., K. Porath, E. Burkel, and U. van Rienen, "Extraction of effective permittivity and permeability of metallic powders in the microwave range," *Model. Simul. Mater. Sci. Eng.*, Vol. 18, 025015–025028, 2010.
17. Lomayeva, S. F., A. V. Syugaev, A. N. Maratkanova, and A. A. Shakov, "Structure and microwave properties of Fe powders prepared by surfactant-assisted ball milling in organic media," *J. Alloys Compd.*, Vol. 721, 18–27, 2017.
18. Ignatenko, M., M. Tanaka, and M. Sato, "Absorption of microwave energy by a spherical nonmagnetic metal particle," *Jap. J. Appl. Phys.*, Vol. 48, No. 6R, 67001–67006, 2009.
19. Sihvola, A. H., "Mixing rules," *Artificial Materials Handbook*, Vol. I: ed. F. Capolino, 9.1–9.12, CRC press, Taylor & Francis, 2009.
20. Sihvola, A. H. and J. Au. Kong, "Effective permittivity of dielectric mixtures," *IEEE Trans. on Geoscience and Remote Sensing*, Vol. 26, No. 4., Jul. 1988.

21. Bergman, D. J., "Bounds for the complex dielectric constant of a two component material," *Phys. Rev. B*, Vol. 23 3058-65, 1981.
22. Zhang, D. and E. Cherkhev, "Reconstruction of spectral function from effective permittivity of a composite material using rational function approximations" *Journal of Computational Physics*, Vol. 228, 5390–5409, 2009.
23. Ghosh, K. and R. Fuchs, "Spectral theory for two-component porous media," *Phys Rev. B*, Vol. 38, No. 8, 5222–5236, 1988.
24. Rozanov, K. N., M. Y. Koledintseva, and J. Drewniak, "A mixing rule for predicting frequency dependence of material parameters in magnetic composites," *J. Magn. Magn. Mater.*, Vol. 324, 1063–1066, 2012.
25. Osipov, A. V., K. N. Rozanov, N. A. Simonov, and S. N. Starostenko, "Reconstruction of intrinsic parameters of a composite from the measured frequency dependence of permeability," *J. Phys. Condens. Matter.*, Vol. 14, 9507–9523, 2002.
26. Rozanov, K. N., A. V. Osipov, D. A. Petrov, S. N. Starostenko, and E. P. Yelsukov, "The effect of shape distribution of inclusions on the frequency dependence of permeability in composites," *J. Magn. Magn. Mater.*, Vol. 321, 738–741, 2009.
27. Petrov, D. A., K. N. Rozanov, and M. Y. Koledintaeva, "Influence of higher-order modes in coaxial waveguide on measurements of material parameters," *IEEE Trans. EMC*, Vol. 3, 66–70, 2018.
28. Arkadiev, W., "Absorption of electromagnetic waves in two parallel wires," *Ann. Physik*, Vol. 58, No. 4, 105–138, 1919.
29. Simon, I., "Magnetic permeability of nickel in the region of centimeter waves," *Nature*, No. 3996, 735, 1946.